December 2006

Autocatalytic Activation of Influenza Hemagglutinin

Jeong H. Lee
University of Pennsylvania

Mark Goulian
University of Pennsylvania

Eric T. Boder
University of Pennsylvania, boder@seas.upenn.edu

Postprint version. Published in *Journal of Molecular Biology*, Volume 364, Issue 3, December 2006, pages 275-282.
Publisher URL: http://dx.doi.org/10.1016/j.jmb.2006.09.015

Autocatalytic Activation of Influenza Hemagglutinin

Abstract
Enveloped viruses contain surface proteins that mediate fusion between the viral and target cell membranes following an activating stimulus. Acidic pH induces the influenza virus fusion protein hemagglutinin (HA) via irreversible refolding of a trimeric conformational state leading to exposure of hydrophobic fusion peptides on each trimer subunit. Herein, we show that cells expressing fowl plague virus HA demonstrate discrete switching behavior with respect to the HA conformational change. Partially activated states do not exist at the scale of the cell, activation of HA leads to aggregation of cell surface trimers, and newly synthesized HA refold spontaneously in the presence of previously activated HA. These observations imply a feedback mechanism involving self-catalyzed refolding of HA and thus suggest a mechanism similar to the autocatalytic refolding and aggregation of prions.

Keywords
cooperative activation, HA, hemagglutinin, influenza, autocatalysis

Comments
Postprint version. Published in *Journal of Molecular Biology*, Volume 364, Issue 3, December 2006, pages 275-282.
Publisher URL: http://dx.doi.org/10.1016/j.jmb.2006.09.015

Autocatalytic Activation of Influenza Hemagglutinin

Jeong H. Lee[1], Mark Goulian[2,4], & Eric T. Boder[1,3,4]*

[1]*Department of Chemical and Biomolecular Engineering, University of Pennsylvania, 220 South 33rd Street, Philadelphia, PA 19104, USA*

[2]*Department of Physics, University of Pennsylvania, 209 South 33rd Street, Philadelphia, PA 19104, USA*

[3]*Department of Bioengineering, University of Pennsylvania, 3320 Smith Walk, Philadelphia, PA 19104, USA.*

[4]*Institute for Medicine and Engineering, University of Pennsylvania, 3340 Smith Walk, Philadelphia, PA 19104, USA.*

**Corresponding author. 220 South 33rd Street, Philadelphia, PA 19104.*

Telephone: (215) 898-5658. Fax: (215) 573-2093. Email: boder@seas.upenn.edu

Enveloped viruses contain surface proteins that mediate fusion between the viral and target cell membranes following an activating stimulus. Acidic pH induces the influenza virus fusion protein hemagglutinin (HA) via irreversible refolding of a trimeric conformational state leading to exposure of hydrophobic fusion peptides on each trimer subunit. Herein, we show that cells expressing fowl plague virus HA demonstrate discrete switching behavior with respect to the HA conformational change. Partially activated states do not exist at the scale of the cell, activation of HA leads to aggregation of cell surface trimers, and newly synthesized HA refold spontaneously in the presence of previously activated HA. These observations imply a feedback mechanism involving self-catalyzed refolding of HA and thus suggest a mechanism similar to the autocatalytic refolding and aggregation of prions.

Keywords: cooperative activation, HA, hemagglutinin, influenza, autocatalysis

Abbreviations used: HA, hemagglutinin; FPV, fowl plague virus; DTT, dithiothreitol; IRES, internal ribosome entry site; CMV, cytomegalovirus

Membrane fusion is an important step in many biological activities, and numerous studies have been performed to investigate fusion protein function[1-4]. Fusion protein activity is required in all infections by enveloped viruses, including influenza viruses. Influenza, an orthomyxovirus, is surrounded by a lipid bilayer membrane envelope captured from the plasma membrane of the cell that generated it, and infection of a host cell involves binding to cell surface sialic acid-containing glycoproteins followed by internalization into endosomal vesicles. Thus, two membranes (viral and endosomal) separate the viral genome from the cell cytoplasm. Viral genetic material is passed through these barriers to the cytosol by fusion of the viral and endosomal membranes, a thermodynamically unfavorable process in the absence of additional energy release[5]. Fusion is promoted by the HA protein, which undergoes a dramatic, irreversible conformational rearrangement following exposure to the low pH of the acidified endosome[6]. Viral fusion proteins, including HA, contain highly conserved hydrophobic peptide segments of ~20 amino acids that are essential to fusion activity[1, 6]. Current models suggest that these fusion peptides spontaneously insert into either the target or viral membrane upon exposure[3], and, along with other conformational alterations of the protein, disrupt membrane structure to allow fusion.

HA is a homotrimer of heterodimer subunits; each HA subunit is synthesized as a single polypeptide (HA0) and proteolytically cleaved into disulfide-linked HA1 and HA2 subunits[7-9]. The x-ray crystal structures of neutral pH (inactive) and pH-activated HA fragments indicate that the fusion peptide relocates from a site largely buried within the trimer to the membrane-distal end of the structure upon activation[6, 10]. Experimental evidence indicates this refolding pathway contains reversible intermediate steps[10-13], and cooperative interaction among adjacent trimers is believed to promote the irreversible transition to the final fusion-competent, refolded state[14-18]. These observations are consistent with the putative requirement for synchronized energy release

via conformational change of multiple HA trimers to overcome the thermodynamic barrier to membrane fusion[5].

Assay of HA refolding decoupled from membrane fusion

We have developed a mammalian expression system where the conformational change of HA from the H7N1 antigenic subtype fowl plague virus A/FPV/Rostock/34 (FPV), can be detected easily and quantitatively by immunofluorescence. A ten amino acid epitope tag sequence (c-myc) was substituted for the C-terminal half of the 20 amino acid FPV fusion peptide (Figure 1a and b), thereby generating a presumably nonfusogenic mutant HA (designated HA3.1) with a conveniently detectable tag potentially sensitive to the activation state of the protein. Cell surface HA (both tagged mutant and wild-type) expressed on transiently transfected NIH-3T3 fibroblasts was analyzed by flow cytometry. Immunofluorescent staining with an anti-HA1 monoclonal antibody demonstrated indistinguishable expression levels of the HA3.1 mutant and wild-type HA (data not shown). The mutant HA also showed irreversible, pH-induced exposure of the epitope tag indistinguishable from pH-induced activation of wild-type HA (Figure 1c), and pH-activated mutant HA were quantitatively sensitive to thermolysin digestion (0.1 mg/mL), which removes the first 23 residues of the HA2 subunit[19], and reduction of the HA1-HA2 intrachain disulfide bond (data not shown). Non-activated mutant HA were insensitive to thermolysin or DTT, consistent with the behavior of wild-type HA from various influenza strains[17]. Two alternative mutants constructed with the epitope tag in the first 11 fusion peptide residues expressed but failed to demonstrate c-myc tag exposure at any tested pH (data not shown), possibly due to inhibition of proteolytic cleavage of the HA0 form, the necessity of fusion peptide residues 1 - 11 in the activation, or perturbation of interactions

between these residues and the charged pocket of the HA1 subunit[20]. Varying the pH of the activating pulse applied to the cells yielded transitions dependent upon the length of the pulse, as expected for an irreversible process (Figure 1c).

Cell-scale synchronization of HA activation

Surprisingly, we observed that transfected cells subjected to pH pulses in the transition region (i.e., partially activated states of the system) demonstrate a strict bimodal response at the cell population level in the case of both tagged mutant and wild-type HA (Figure 1d - g). While fewer cells are activated by higher pH pulses, cell response is rigorously two-state; the intermediate states of the system (i.e., cells activated at intermediate pH or for intermediate duration) include no cells with intermediate levels of c-myc epitope exposure or loss of HC58 reactivity, but rather a mixture of cells with fully non-activated or fully refolded HA. In addition, no cells are positive for both c-myc tag exposure and preinduction conformation (Figure 1g). Thus, no cell exists in a state in which only a fraction of its inducible HA trimers have proceeded through the irreversible conformational change. This striking result indicates that individual cells reach a critical threshold beyond which all activation-competent HA trimers on the cell are irreversibly committed to refolding, implying either cooperative activity on a massive scale or an alternative mechanism such as autocatalysis is involved in the refolding pathway.

Density dependence of HA refolding

Concerted activation of FPV HA proceeding to completion following reversal of the pH pulse implies intertrimer interactions and thus a dependence on trimer cell surface density. To

further investigate this phenomenon, we quantitatively analyzed density dependence using the flow cytometric data of Figure 1e - f. As the acidity or duration of the activating pulse increased, cells with decreasing levels of surface-expressed HA were activated (Figure 1e - f and Figure 2), consistent with the behavior of HA from other antigenic subtype strains as observed via bulk biochemical assays[16, 17, 21], which yield data averaged over cell or virus populations. Analysis of activation lag times as a function of surface expression density suggests lag time converges to ~2.5 min at high HA density (Figure 2c).

Activation-induced HA aggregation

The pre- and post-activation spatial localization of FPV HA were examined by fluorescence microscopy (Figure 3). Cells expressing either wild-type or c-myc-tagged FPV HA demonstrate distributed anti-HA staining prior to an activating pulse, while acid-pulsed cells demonstrate substantial aggregation of HA. Thus, pH-induced refolding of HA appears to coincide with aggregation of refolded trimers, in agreement with previous observations of pH-induced morphological alteration and mobility restriction of HA from another influenza strain[5, 19, 22]. HA3.1-expressing cells activated at intermediate pH and costained for both HA3.1 protein and exposed c-myc tag demonstrate the expected discrete activation phenomenon, and exposed c-myc tags co-localize with aggregated HA3.1 protein (Figure 3c). In accord with flow cytometry data, partially activated cell populations show cells positive for either aggregated and exposed c-myc tags or distributed and nonrefolded HA3.1, with no coincidence of the two phenotypes (Figure 3d).

Autocatalytic refolding of HA dependent on fusion peptide

What mechanism might explain the observed phenomena? Intertrimer cooperativity leading to tandem refolding of trimer aggregates is consistent with density dependence; however, this model predicts that partially-induced intermediate states, in which only a fraction of cooperative units on a given cell are refolded, should exist at the cell scale assuming the cooperative unit is smaller than the number of trimers expressed. We observe no such intermediate states in a large statistical sampling by flow cytometry, as indicated by the lack of intermediate cell populations demonstrating c-myc staining decorrelated from expression level (Figure 1d-f). The absence of partially activated cellular intermediates would thus suggest that the minimal cooperative unit contains all trimers on the cell surface; however, this model then raises the question as to how the cooperative unit could vary dramatically between two cells expressing HA at levels differing by >10-fold, as seen here (e.g., Figure 1e). We observe no stable (i.e., equilibrated) cell populations where high expressers are activated while those of low expression density are not, suggesting the critical cooperative unit size must be less than the minimum observable trimer expression level in the transfected cell population. Our observation that refolding of FPV HA trimers on a cell proceeds irreversibly to a fully activated state, regardless of expression density, therefore argues that cooperative activation cannot fully explain the phenomenon.

The simplest model consistent with these data includes a positive feedback mechanism by which irreversibly activated FPV HA trimers (which may result from an event involving a small cooperative unit) promote the irreversible refolding of non-activated trimers (Figure 4a). This model accounts for the observed irreversible commitment to refolding at the cell scale; once one

or more trimers become irreversibly refolded, the feedback chain reaction proceeds until all remaining activatable trimers have refolded, despite removal of the activating pH stimulus.

To more directly test this model, we pulsed cells expressing low levels of HA prior to further culturing to allow synthesis and secretion of additional HA that had not been exposed to the inducing low pH pulse. At both 8 h (Figure 4b, c) and 20 h (data not shown) after the inducing pH pulse, HA3.1-expressing cells demonstrated increased HA levels and a correlated increase in c-myc tag exposure. Similarly, wild-type HA-expressing cells demonstrated increased HA levels 8 h after an inducing pH pulse, yet the new HA failed to react with trimer-specific mAb HC58 (Figure 4e), indicating it had adopted the activated conformation. Thus, new HA expressed during the post-pulse culturing refolded spontaneously, supporting the model that refolding was catalyzed by the previously refolded HA already present on the cell. Furthermore, treatment of pH-pulsed cells with thermolysin prior to reculturing quantitatively cleaved the fusion peptide/c-myc tag region and abolished spontaneous refolding of newly synthesized HA (both HA3.1 and wild-type HA), while the new HA remained inducible by a subsequent acid pulse (Figure 4d, e). In contrast, trypsin treatment (20 μg/mL, 15 min at 37 °C) of pH pulsed cells (which is expected to cleave the HA1 domain[19]) had no effect on spontaneous HA3.1 refolding following an additional 8 h in culture (data not shown). FPV HA was previously shown to refold in the acidic Golgi compartment when expressed in CV-1 cells, and this refolding was inhibited by acidotropic agents such as amantidine and NH_4Cl[23], which buffered the intracellular pH. The formal possibility therefore exists that pH pulsing 3T3 cells might alter intracellular pH to induce HA refolding several hours later, and that thermolysin might inhibit this effect in some manner. Repeating experiments with 3T3 cells maintained in the presence of 10 mM NH_4Cl at all stages except the pH 5 pulse, however, yielded results

identical to those of Figure 4c (data not shown), suggesting alteration of intracellular pH is not responsible for the phenomenon. Taken together, these data suggest that the fusion peptide region, and perhaps its effect on the local membrane environment, is necessary for autocatalytic refolding.

Autocatalysis of HA refolding could result from either direct trimer-trimer interaction or from effects mediated by locally altered membrane structure and tension. Either mechanism suggests the necessity of physical interaction or proximity between refolded and nonrefolded trimers and thus is consistent with the observed activation-correlated aggregation (Figure 3). The relative timing of aggregation versus irreversible refolding, however, has yet to be determined for this system, and thus a direct link between autocatalytic refolding and aggregation has not been established. Nonetheless, it is conceivable that trimer refolding could be linked to incorporation into a central protein aggregate or an expanding ring of perturbed membrane structure. The speculation that altered membrane tension might induce refolding is consistent with the membrane destabilization required to induce fusion with a juxtaposed target membrane and has been previously proposed[17]. This mechanism would coordinate conformational energy release of a large number of HA trimers and lead to a domain of high-energy membrane structure. Indeed, a similar mechanism involved in HA-mediated membrane fusion has been previously suggested[5], and Leikina, et al., recently demonstrated that HA trimers from outside the intercellular contact zone are necessary for fusion pore expansion[24], consistent with a requirement for activated HA aggregation. Insertion of exposed fusion peptides into the cell membrane (or N-terminal 11 residues of the fusion peptide in the HA3.1 mutant) could alter membrane tension and curvature with resulting effects on trimer conformational stability; membrane tension has been previously observed to impact folded stability of bacterial outer

membrane protein A[25]. This supposition is also consistent with the suggested structure of membrane-embedded HA fusion peptide[26-29], in which the N-terminal portion of the fusion peptide embeds into the nonpolar membrane core and disrupts lipid structure. However, despite the observed thermolysin sensitivity of the autocatalytic refolding, direct evidence for membrane involvement in this phenomenon and for the existence of autocatalytic HA refolding in the context of intermembrane fusion require further studies.

Prion-like refolding behavior

Our proposed model for refolding of FPV HA to the fusion-active conformation parallels the hypothesized refolding feedback mechanism by which infectious proteins (prions) induce irreversible refolding and aggregation of structural isoforms[30], and the fusion peptide of HA demonstrates sequence similarity to amyloid β peptide and a prion sequence[31-33]. To our knowledge, this is the first example of data consistent with such a mechanism for conformational regulation putatively involved in the function of a membrane protein. Whether this phenomenon applies to other viral fusion proteins, or to other membrane proteins functionally dependent upon conformational changes, remains to be investigated. Nonetheless, the existence of autocatalytic. pH-induced refolding of FPV hemagglutinin raises interesting possibilities regarding the understanding of conformational molecular switches.

Acknowledgments

We thank Dr. Hans-Dieter Klenk for providing the anti-FPV HA serum, Dr. Steve Wharton for anti-FPV HA mAbs HC2 and HC58, and Dr. Paula Cannon for the cloned FPV HA gene. Funding was provided by NSF NIRT 02-10777.

References

1. Eckert, D. M. & Kim, P. S. (2001). Mechanisms of Viral Membrane Fusion and Its Inhibition. *Annu Rev Biochem* **70**, 777-810.
2. Blumenthal, R., Clague, M. J., Durell, S. R. & Epand, R. M. (2003). Membrane fusion. *Chem Rev* **103**, 53-69.
3. Jahn, R., Lang, T. & Sudhof, T. C. (2003). Membrane fusion. *Cell* **112**, 519-533.
4. Chen, E. H. & Olson, E. N. (2005). Unveiling the mechanisms of cell-cell fusion. *Science* **308**, 369-373.
5. Chernomordik, L. V. & Kozlov, M. M. (2003). Protein-lipid interplay in fusion and fission of biological membranes. *Annu Rev Biochem* **72**, 175-207.
6. Skehel, J. J. & Wiley, D. C. (2000). Receptor binding and membrane fusion in virus entry: the influenza hemagglutinin. *Annu Rev Biochem* **69**, 531-569.
7. Huang, R. T., Rott, R. & Klenk, H. D. (1981). Influenza viruses cause hemolysis and fusion of cells. *Virology* **110**, 243-247.
8. Huang, R. T., Wahn, K., Klenk, H. D. & Rott, R. (1980). Fusion between cell membrane and liposomes containing the glycoproteins of influenza virus. *Virology* **104**, 294-302.
9. Klenk, H. D., Rott, R., Orlich, M. & Blodorn, J. (1975). Activation of influenza A viruses by trypsin treatment. *Virology* **68**, 426-439.
10. White, J. M. & Wilson, I. A. (1987). Anti-peptide antibodies detect steps in a protein conformational change: low-pH activation of the influenza virus hemagglutinin. *J Cell Biol* **105**, 2887-2896.
11. Korte, T., Ludwig, K., Booy, F. P., Blumenthal, R. & Herrmann, A. (1999). Conformational intermediates and fusion activity of influenza virus hemagglutinin. *J Virol* **73**, 4567-4574.

12. Korte, T., Ludwig, K., Krumbiegel, M., Zirwer, D., Damaschun, G. & Herrmann, A. (1997). Transient changes of the conformation of hemagglutinin of influenza virus at low pH detected by time-resolved circular dichroism spectroscopy. *J Biol Chem* **272**, 9764-9770.

13. Tatulian, S. A. & Tamm, L. K. (1996). Reversible pH-dependent conformational change of reconstituted influenza hemagglutinin. *J Mol Biol* **260**, 312-316.

14. Krumbiegel, M., Herrmann, A. & Blumenthal, R. (1994). Kinetics of the low pH-induced conformational changes and fusogenic activity of influenza hemagglutinin. *Biophys J* **67**, 2355-2360.

15. Leikina, E., Ramos, C., Markovic, I., Zimmerberg, J. & Chernomordik, L. V. (2002). Reversible stages of the low-pH-triggered conformational change in influenza virus hemagglutinin. *EMBO J* **21**, 5701-5710.

16. Danieli, T., Pelletier, S. L., Henis, Y. I. & White, J. M. (1996). Membrane fusion mediated by the influenza virus hemagglutinin requires the concerted action of at least three hemagglutinin trimers. *J Cell Biol* **133**, 559-569.

17. Markovic, I., Leikina, E., Zhukovsky, M., Zimmerberg, J. & Chernomordik, L. V. (2001). Synchronized activation and refolding of influenza hemagglutinin in multimeric fusion machines. *J Cell Biol* **155**, 833-844.

18. Bentz, J. (2000). Minimal aggregate size and minimal fusion unit for the first fusion pore of influenza hemagglutinin-mediated membrane fusion. *Biophys J* **78**, 227-245.

19. Ruigrok, R. W., Wrigley, N. G., Calder, L. J., Cusack, S., Wharton, S. A., Brown, E. B. & Skehel, J. J. (1986). Electron microscopy of the low pH structure of influenza virus haemagglutinin. *EMBO J* **5**, 41-49.

20. Steinhauer, D. A. (1999). Role of hemagglutinin cleavage for the pathogenicity of influenza virus. *Virology* **258**, 1-20.

21. Clague, M. J., Schoch, C. & Blumenthal, R. (1991). Delay time for influenza virus hemagglutinin-induced membrane fusion depends on hemagglutinin surface density. *J Virol* **65**, 2402-2407.

22. Gutman, O., Danieli, T., White, J. M. & Henis, Y. I. (1993). Effects of exposure to low pH on the lateral mobility of influenza hemagglutinin expressed at the cell surface: correlation between mobility inhibition and inactivation. *Biochemistry* **32**, 101-106.

23. Ohuchi, M., Cramer, A., Vey, M., Ohuchi, R., Garten, W. & Klenk, H. D. (1994). Rescue of vector-expressed fowl plague virus hemagglutinin in biologically active form by acidotropic agents and coexpressed M2 protein. *J Virol* **68**, 920-926.

24. Leikina, E., Mittal, A., Cho, M. S., Melikov, K., Kozlov, M. M. & Chernomordik, L. V. (2004). Influenza hemagglutinins outside of the contact zone are necessary for fusion pore expansion. *J Biol Chem* **279**, 26526-26532.

25. Hong, H. & Tamm, L. K. (2004). Elastic coupling of integral membrane protein stability to lipid bilayer forces. *Proc Natl Acad Sci U S A* **101**, 4065-4070.

26. Han, X., Bushweller, J. H., Cafiso, D. S. & Tamm, L. K. (2001). Membrane structure and fusion-triggering conformational change of the fusion domain from influenza hemagglutinin. *Nat Struct Biol* **8**, 715-720.

27. Lague, P., Roux, B. & Pastor, R. W. (2005). Molecular dynamics simulations of the influenza hemagglutinin fusion Peptide in micelles and bilayers: conformational analysis of Peptide and lipids. *J Mol Biol* **354**, 1129-1141.

28. Vaccaro, L., Cross, K. J., Kleinjung, J., Straus, S. K., Thomas, D. J., Wharton, S. A., Skehel, J. J. & Fraternali, F. (2005). Plasticity of influenza haemagglutinin fusion peptides and their interaction with lipid bilayers. *Biophys J* **88**, 25-36.

29. Huang, Q., Chen, C. L. & Herrmann, A. (2004). Bilayer conformation of fusion peptide of influenza virus hemagglutinin: a molecular dynamics simulation study. *Biophys J* **87**, 14-22.

30. Weissmann, C. (2005). Birth of a prion: spontaneous generation revisited. *Cell* **122**, 165-168.

31. Forloni, G., Angeretti, N., Chiesa, R., Monzani, E., Salmona, M., Bugiani, O. & Tagliavini, F. (1993). Neurotoxicity of a prion protein fragment. *Nature* **362**, 543-546.

32. Del Angel, V. D., Dupuis, F., Mornon, J. P. & Callebaut, I. (2002). Viral fusion peptides and identification of membrane-interacting segments. *Biochem Biophys Res Commun* **293**, 1153-1160.

33. Crescenzi, O., Tomaselli, S., Guerrini, R., Salvadori, S., D'Ursi, A. M., Temussi, P. A. & Picone, D. (2002). Solution structure of the Alzheimer amyloid beta-peptide (1-42) in an apolar microenvironment. Similarity with a virus fusion domain. *Eur J Biochem* **269**, 5642-5648.

34. Lin, A. H., Kasahara, N., Wu, W., Stripecke, R., Empig, C. L., Anderson, W. F. & Cannon, P. M. (2001). Receptor-specific targeting mediated by the coexpression of a targeted murine leukemia virus envelope protein and a binding-defective influenza hemagglutinin protein. *Hum Gene Ther* **12**, 323-332.

35. Sauter, N. K., Hanson, J. E., Glick, G. D., Brown, J. H., Crowther, R. L., Park, S. J., Skehel, J. J. & Wiley, D. C. (1992). Binding of influenza virus hemagglutinin to analogs of its cell-surface receptor, sialic acid: analysis by proton nuclear magnetic resonance spectroscopy and X-ray crystallography. *Biochemistry* **31**, 9609-9621.

36. Sugrue, R. J., Bahadur, G., Zambon, M. C., Hall-Smith, M., Douglas, A. R. & Hay, A. J. (1990). Specific structural alteration of the influenza haemagglutinin by amantadine. *EMBO J* **9**, 3469-3476.

Figure Captions

Figure 1. Functional analysis of wild-type and HA3.1 mutant hemagglutinin and density dependence of c-myc induction. (**a**) The c-myc epitope tag sequence (underlined) replaced a 10 amino acid sequence of the fusion pepide. A Kozak sequence GCCACC was added to the wild-type FPV HA gene[34] (from A/FPV/Rostock/34) by PCR in order to increase the expression in mammalian cells. Amino acids 343 to 352, 344 to 353, or 353 to 362 (i.e., fusion peptide residues 1 - 10, 2 - 11, or 11 - 20) were replaced with the c-myc epitope tag sequence via PCR using a SalI site introduced by a silent mutation just upstream of the fusion peptide region. Wild-type HA and the mutants were cloned into a pIRES (BD Biosciences, Mountain View, CA) based mammalian expression vector containing the CMV promoter after the IRES sequence was removed. (**b**) Structural rendering of X-31 HA (homologous to FPV HA) highlighting the location of the fusion peptide in the preactivation conformation. Fusion peptide residues 1 - 10 are colored blue and 11 - 20 (mutated in HA3.1) are colored red. Coordinates used in the analysis are from PDB file 1HGF[35], and the images were generated using MacPyMOL software (http://www.pymol.org). (**c**) Cells were transfected using Lipofectamine 2000 (Invitrogen, Carlsbad, CA) following the manufacturer's protocol. For negative control experiments, one well was transfected with empty pIRES vector. Transfection efficiency was monitored by parallel transfection with gWiz-GFP (Gene Therapy Systems, San Diego, CA). Adherent, nonconfluent HA3.1 (filled symbols) or wild-type HA (open symbols) vector transient transfectants (24 h post-transfection) were pH-pulsed for 2 min or 5 min at room temperature. HA3.1 cells were double-stained with rabbit polyclonal anti-FPV HA and anti-c-myc mAb 9E10 (Covance, Berkeley, CA), and wild-type HA cells were double-stained with biotinylated anti-HA1 mAb HC2 and conformation-specific anti-HA1 mAb HC58 (specific for trimeric HA1 in

the preactivation conformation)[36]. HC2 mAb was purified from ascites fluid using Protein G-agarose (Invitrogen, Carlsbad, CA) and biotinylated using the EZ-Link NHS-PEO4-Biotinylation Kit (Pierce, Rockford, IL) following the manufacturer's protocol. Only viable cells, as determined by propidium iodide exclusion and/or light scattering, were included in the analysis by flow cytometry, and 20,000 gated events were analyzed for all flow cytometric experiments. The fraction of HA3.1-expressing cells positive for the c-myc epitope or the fraction of wild-type HA-expressing cells negative for HC58 is shown. Data represents averages of four independent experiments and error bars represent standard deviation. **(d)** Wild-type HA-expressing cells (WT HA) were pulsed at the indicated pH for 5 min at room temperature, washed with pH 7.4 buffer, co-stained with biotin-HC2 and HC58, and analyzed by flow cytometry. Fractions of the total viable cell population falling within the indicated regions of the two-color histograms are indicated. (**e)** HA3.1-expressing cells were pulsed at the indicated pH for 5 min or **(f)** pulsed at pH 5.0 for the indicated time at room temperature and costained with rabbit anti-HA and anti-c-myc. (**g**) HA3.1-expressing cells were pulsed at the indicated pH for 5 min at room temperature, costained with HC58 and chicken anti-c-myc (Jackson ImmunoResearch Laboratory, West Grove, PA), and analyzed by flow cytometry.

Figure 2. Expression density dependence of HA induction. Flow cytometry data were gated at various levels of anti-HA staining intensity (minimum region width set to maintain at least 100 gated events for all data points) using CellQuest software (Becton-Dickinson, Franklin Lakes, NJ) to allow calculation of (**a**) the fraction of cells induced as a function of relative HA expression density for pulse durations of 0 min (◆), 3.0 min (✳), 3.5 min (■), 4.0 min (▲) and 4.5 min (●), or (**b**) the fraction of cells induced as a function of pulse time for HA expression

densities at normalized mean fluorescence intensities of 2.28 (◆), 25.85 (●), 80.33 (■) and 204.43 (▲). A dose-response equation was fit to the data with two adjustable parameters (pulse time required for 50% of the cell population to be induced [T50] and inflection slope). The minimum R^2 value of the fitted curves was 0.9875. (**c**) T50 values calculated from three separate experiments were averaged and plotted as a function of relative HA expression density. Vertical error bars represent standard deviation of the three values and horizontal error bars represent standard deviation of the average corrected MFL of cells within a density gate from three experiments. Absence of error bars indicates range is less than the width of the symbol. The mean fluorescence intensity (MFL) for each gate was corrected by subtracting the mean background auto-fluorescence intensity of a stained negative control population.

Figure 3. Aggregation of HA following pH pulse. (**a**) Live HA3.1-expressing or wild-type HA-expressing fibroblasts were immunofluorescently stained with anti-c-myc antibody (HA3.1) or anti-HA serum (WT HA) following a 5 min pulse at pH 5.0 and room temperature and analyzed at 20X magnification on a Nikon ECLIPSE ES300 inverted fluorescence microscope. (**b**) HA3.1 or wild-type HA-expressing cells were stained with anti-HA serum following a 5 min pulse at the indicated pH and room temperature and analyzed at 64X magnification on an Olympus IX71 inverted fluorescence microscope. (**c**) HA3.1 expressing cells were costained with anti-c-myc/goat anti-mouse-TRITC (red) followed by biotin-HC2/streptavidin-FITC (green) following a 5 min pulse at pH 5.4 (room temperature) and analyzed at 40X magnification on an Olympus IX71 inverted fluorescence microscope. FITC and TRITC fluorescence images were overlayed using NIH ImageJ v1.36 (http://rsb.info.nih.gov/ij/). (**d**) Cells were pulsed at pH 5.4 for 5 min at room temperature 24 h post-transfection, costained with biotin-HC58/streptavidin-

FITC (BD Biosciences, San Diego, CA) and 9E10/anti-mouse-TRITC (Sigma, St. Louis, MO) , and analyzed as in (c).

Figure 4. Fusion peptide-dependent autocatalytic refolding. **(a)** A possible refolding reaction pathway for FPV HA is diagrammed. Acidic pH-activated, refolded HA catalyzes refolding of non-activated HA directly or through alteration of lipid bilayer structure and membrane tension. Steps in the shaded region represent putative intermediates suggested in studies of X-31 HA[12-15] and include exposure of the fusion peptide and clustering into cooperative units (however, reversible intermediates have not been demonstrated for HA from FPV). Cooperative units might include both "primed" and inactive trimers. Data herein implies a positive feedback loop (i.e., an alternative product-catalyzed reaction pathway) must be active regardless of intermediate states in the conformational change. (**b-d)** HA3.1-transfected cells were analyzed by flow cytometry 16 h (at which time cells express low but detectable levels of HA3.1) or 24 h (high expression) after transfection. Filled grey histograms represent empty vector-transfected cells. **(b**) Cells pulsed at 16 h post-transfection and recultured for an additional 8 h were stained with HC2 mAb and analyzed by flow cytometry to confirm increased expression of HA3.1 following reculturing. **(c)** Cells were pulsed at pH 5.0 at 16 h post-transfection. A fraction of the cells were immediately labeled with anti-c-myc antibody and analyzed by flow cytometry. Remaining cells were cultured for an additional 8 h in fresh medium prior to antibody staining and analysis with (P: +) or without (P: -) an additional pH 5 pulse at 24 h post-transfection. **(d)** Cells pH-pulsed at 16 h post-transfection as in (c) were treated with (T: +) or without (T: -) thermolysin (0.1 mg/mL for 30 min at 37 °C; EMD Biosciences, San Diego, CA) to cleave the fusion peptide and a fraction analyzed by anti-c-myc

staining and flow cytometry. Remaining cells were cultured for an additional 8 h prior to staining and analyzed with (P: +) or without (P: -) an additional pH pulse at 24 h post-transfection. (**e**) Cells transfected with wild-type HA vector were treated as in (c) and (d) and analyzed using mAb HC58 specific for nonrefolded HA and mAb HC2 specific for total HA protein to confirm autocatalytic and thermolysin-sensitive refolding of WT protein.

Figure 1

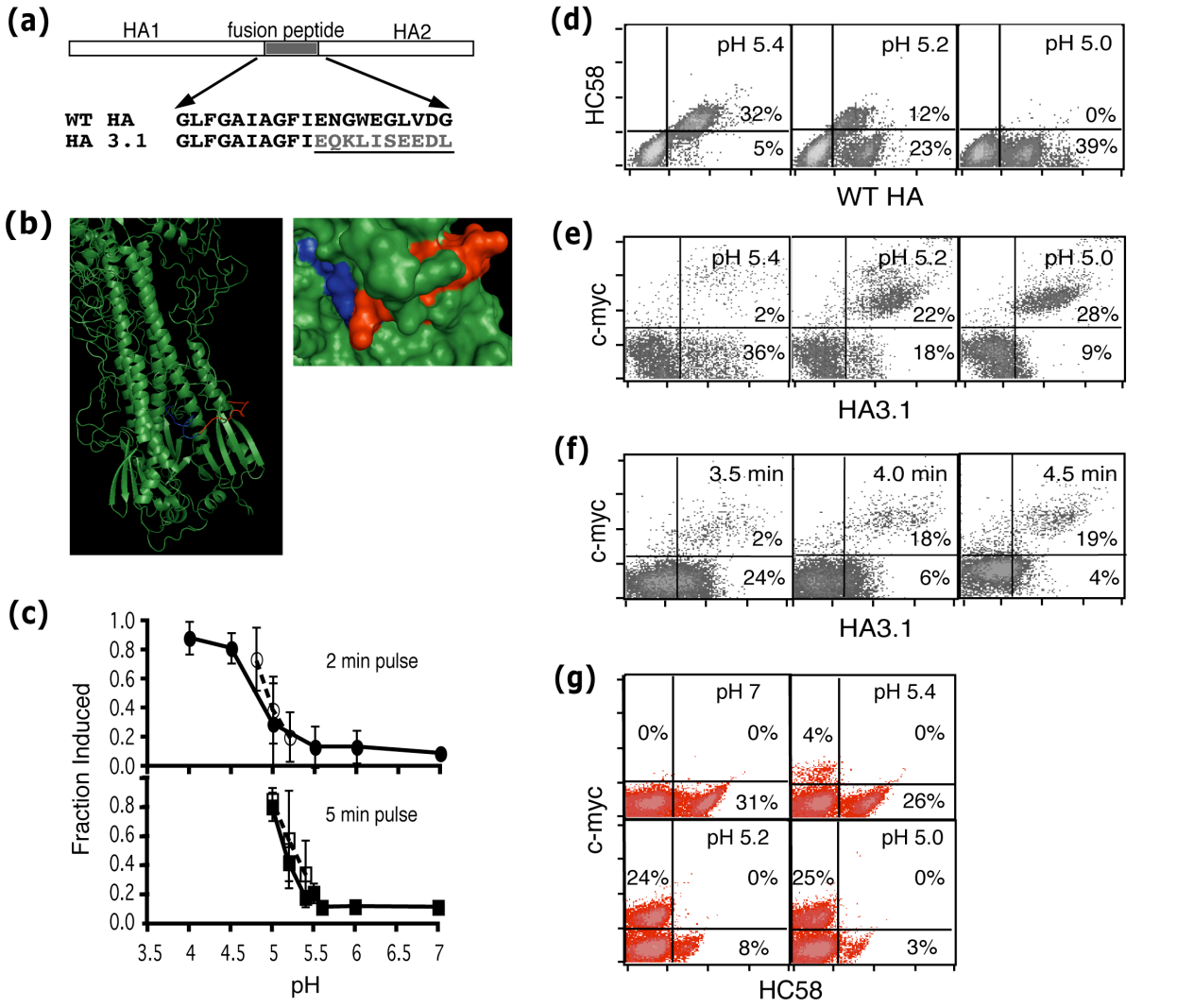
(a)
HA1
fusion peptide
HA2
WT HA GLFGAIAGFIENGWEGLVDG
HA 3.1 GLFGAIAGFIEQKLISEEDL
(b)
(c)
Fraction Induced
2 min pulse
5 min pulse
pH
(d)
HC58
pH 5.4
pH 5.2
pH 5.0
32%
5%
12%
23%
0%
39%
WT HA
(e)
c-myc
2%
36%
22%
18%
28%
9%
HA3.1
(f)
3.5 min
4.0 min
4.5 min
2%
24%
18%
6%
19%
4%
HA3.1
(g)
pH 7
pH 5.4
pH 5.2
pH 5.0
0%
31%
4%
26%
24%
8%
25%
3%
HC58

Figure 2

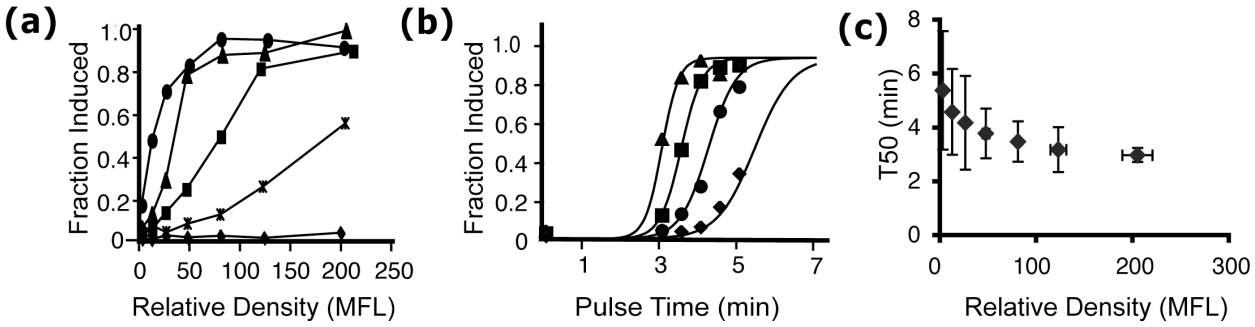
(a)
Fraction Induced
1.0
0.8
0.6
0.4
0.2
0
0 50 100 150 200 250
Relative Density (MFL)
(b)
Fraction Induced
1.0
0.8
0.6
0.4
0.2
0
1 3 5 7
Pulse Time (min)
(c)
T50 (min)
8
6
4
2
0
0 100 200 300
Relative Density (MFL)

Figure 3

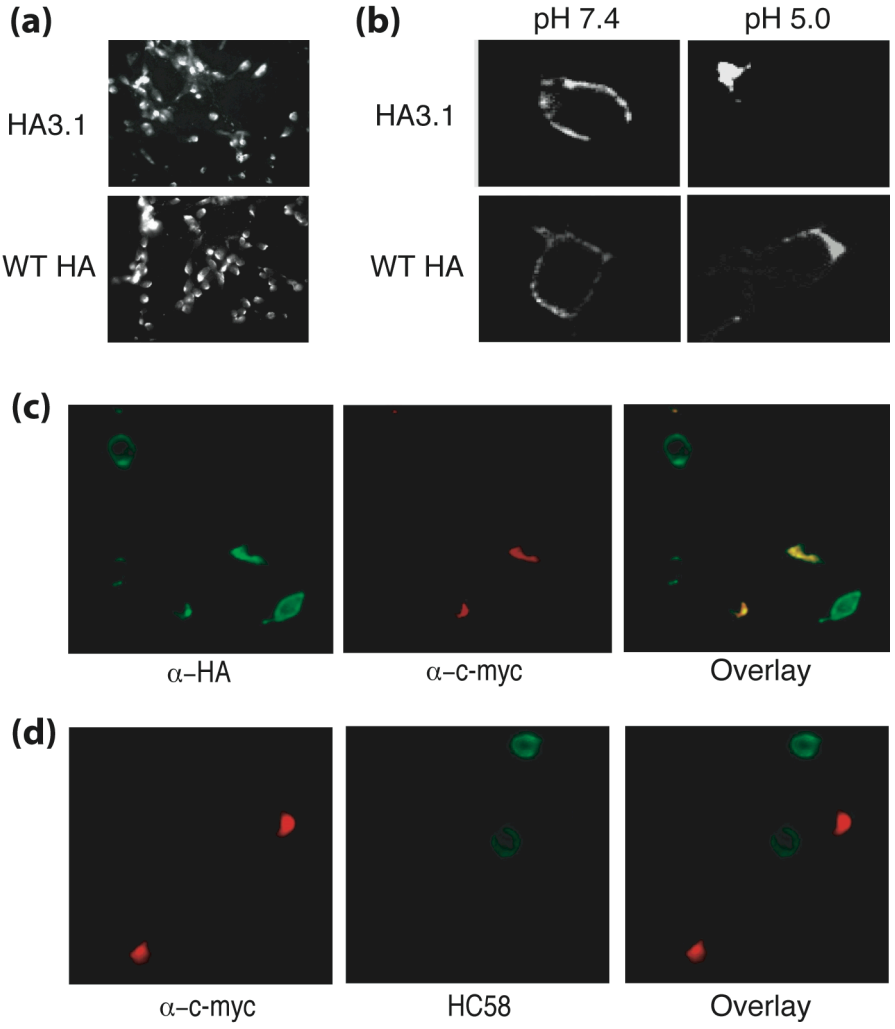
(a)
HA3.1
WT HA
(b)
pH 7.4
pH 5.0
HA3.1
WT HA
(c)
α–HA
α–c-myc
Overlay
(d)
α–c-myc
HC58
Overlay

Figure 4

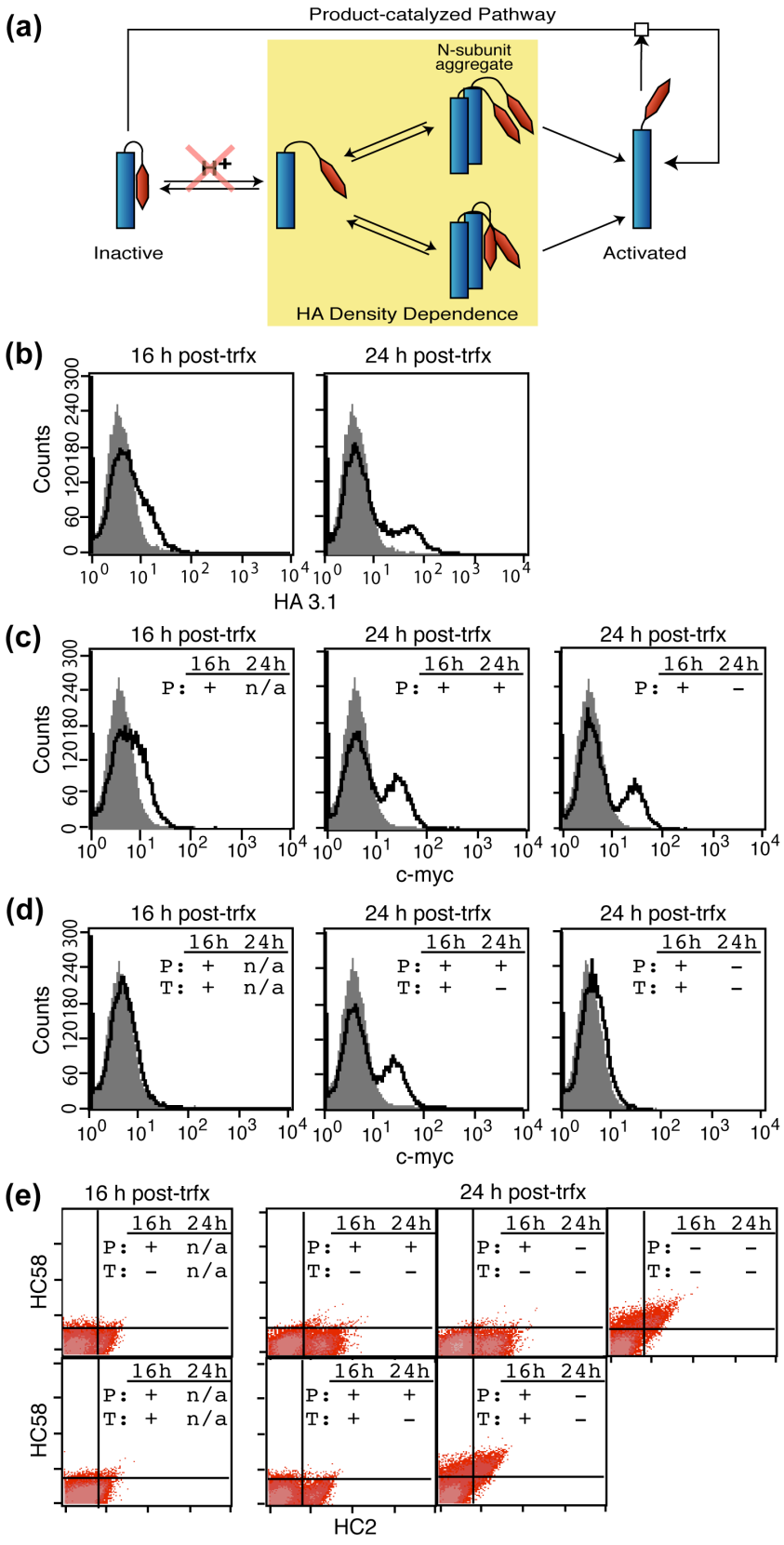
(a)
Product-catalyzed Pathway
N-subunit aggregate
H+
Inactive
Activated
HA Density Dependence
(b)
16 h post-trfx
24 h post-trfx
Counts
HA 3.1
(c)
16h 24h
P: + n/a
P: + +
P: + –
c-myc
(d)
T: + n/a
T: + –
(e)
HC58
HC2